communications earth & environment

Article

https://doi.org/10.1038/s43247-024-01352-4

Projected changes in compound hot-dry events depend on the dry indicator considered

Check for updates

Parisa Hosseinzadehtalaei [1] ✉, Piet Termonia [1,2] & Hossein Tabari [2,3,4]

The intensification of compound hot-dry events due to climate change is a pressing concern, underscoring the need for precise analysis. However, the impact of different dry indicators on projections of these events has not been quantitatively evaluated, nor has its importance been compared with other sources of uncertainty. Here we examine the sensitivity of projected changes in compound hot-dry events to different dry indicators. We use data from 22 Coupled Model Intercomparison Project Phase 6 (CMIP6) models to characterize global dry conditions based on precipitation, runoff, soil moisture, and a multivariate index combining these variables through trivariate copulas. Our findings reveal large differences in projected changes in the likelihood of compound hot-dry events across different dry indicators. While model uncertainty remains the primary source of uncertainty for compound hot-dry event projections, the uncertainty associated with dry indicators is also substantial, surpassing scenario uncertainty in specific regions.

Droughts and heatwaves often occur together due to the influence of both local land-atmosphere feedbacks[1] and large-scale ocean-atmosphere circulations[2,3]. These feedbacks lead to an increase in surface sensible heat from droughts and a subsequent rise in temperature, which can be propagated downwind through heat advection[4,5]. With an increase in the frequency of both heatwaves and droughts[6,7], and stronger land-atmosphere feedback triggered by atmospheric warming[8], compound hot-dry events are becoming more common and severe across different regions of the world[9,10]. These events have substantial adverse impacts on ecosystems, agriculture, water resources, and human health[11–13].

To develop effective strategies for adapting to and mitigating the impacts of these events, it is critical to understand and project their future characteristics. However, defining compound hot-dry events as a new topic in climate change research is a complex task. The choice of dry indicators can drastically impact the projected changes in dry events[14–16], potentially altering the magnitude and even the sign of the projected changes in compound hot-dry events. Such discrepancies can have substantial implications for adaptation and mitigation strategies, as different definitions may require different types of infrastructure investments and spatial planning to prepare for and mitigate the impacts of these events[17]. Therefore, evaluating the impact of different dry indicators on projections of compound events is crucial to ensure that decision-makers have access to accurate and reliable information for effective planning and decision-making.

Dry events in compound hot-dry events in climate change studies have typically been defined based solely on precipitation[18–22], but this may oversimplify the underlying complexities of such events. To better capture these complexities, some studies have incorporated additional variables, such as runoff and soil moisture[8,23]. Recent studies comparing different definitions based on precipitation, runoff, and soil moisture have highlighted large differences in the projected changes in compound hot-dry events and associated uncertainties[24,25]. However, since these variables are interrelated components of the same process[25], it is essential to consider their interactions for accurate projections of compound hot-dry events[26]. Unfortunately, global-scale compound hot-dry event projections that incorporate the interconnections between low precipitation, soil moisture, and runoff are currently lacking.

Properly understanding the uncertainty in future projections of compound hot-dry events is crucial for interpreting the impacts of climate change and making informed policy decisions to mitigate the associated risks[27]. However, while traditional sources of uncertainty in climate change projections such as climate models and scenarios have been well studied[28–31], less attention has been given to uncertainties associated with other factors, including hazard definition. Although recent studies have highlighted the

[1]Department of Physics and Astronomy, Ghent University, Ghent, Belgium. [2]Department of Meteorological and Climate Research, Royal Meteorological Institute of Belgium, Uccle, Belgium. [3]M4S, Faculty of Applied Engineering, University of Antwerp, Antwerp, Belgium. [4]United Nations University Institute for Water, Environment and Health, Hamilton, ON, Canada. ✉e-mail: parisa.hosseinzadehtalaei@ugent.be

importance of including dry event definitions in uncertainty analyses[32,33], its relative significance for compound hot-dry event projections compared with other sources of uncertainty remains unclear. Specifically, there is a lack of understanding regarding how much projected changes in compound hot-dry events can vary depending on dry indicators. Addressing this issue can help quantify the amount of uncertainty that can be reduced by refining the event definition.

To bridge these knowledge gaps, this study aims to project global compound hot-dry events using 22 global climate models (GCMs) from the Coupled Model Intercomparison Project Phase 6 (CMIP6) under four Shared Socioeconomic Pathways (SSPs). The study characterizes compound hot and dry precipitation, soil moisture, and runoff extremes, as well as compound hot and multivariate dry extremes. The study then compares the uncertainties arising from different definitions of dry conditions for compound hot-dry events with those arising from GCMs and SSPs.

Results

Having established that the CMIP6 GCMs have undergone comprehensive evaluations for simulating compound hot-dry events in prior studies[21,24,34,35], our focus remains on investigating how different dry indicators impact projections of compound hot-dry events (Fig. 1). A comparison of changes in the probability of compound hot-dry events, with dry events characterized based on precipitation [HDI-P], runoff [HDI-R], and soil moisture [HDI-S], reveals a similar spatial distribution (Fig. 1). Across all indices, the probability of compound events is projected to increase worldwide by the end of this century under different scenarios. The most substantial increase is anticipated in most of South America, Central America, southern North America, southern and northern Africa, southern and central Europe, western Asia, and Australia. However, the magnitude of the increase in compound event probability noticeably varies among the different indices. Generally, the increase in probability for HDI-P is lower than that for HDI-R and HDI-S, and this disparity is more pronounced in regions expected to experience the most severe impacts from compound events. Based on the CMIP6 ensemble median, the global maximum increase in compound event probability differs noticeably across the various indices, with values ranging from 0.12 to 0.26 for HDI-P, 0.26 to 0.60 for HDI-R, and 0.31 to 0.59 for HDI-S, depending on the scenarios. Although the difference between the increase in probability for HDI-R and HDI-S is small, the increase in probability for HDI-R and HDI-S is consistently 2-3 times larger compared with HDI-P.

In addition to defining dry conditions for compound hot-dry events by linking temperature with various hydrological variables, an alternative approach involves defining compound events based on the combination of these variables, referred to as the HDI-MSDI (Fig. 1). When compound hot-dry events are defined using HDI-MSDI, the projected changes exhibit collective variations in the different hydrological variables, evident in both spatial distribution and magnitude. The spatial pattern of projected changes in the probability of HDI-MSDI closely resembles that of HDI-P, HDI-R, and HDI-S, with similar regions expected to be most impacted. In terms of magnitude, the expected increase in the probability of HDI-MSDI is greater than that of HDI-P, but smaller than that of HDI-R and HDI-S.

The projected changes based on HDI-P, HDI-R, HDI-S, and HDI-MSDI are globally significant at the 5% level (Supplementary Fig. 1). Even when reducing the significance level to 1% and 0.1%, the substantial changes obtained by HDI-P continue to encompass 100% of the global land areas. However, the coverage marginally decreases for the other indices, spanning 95-100% of the land area. Notably, HDI-P yields the highest signal-to-noise ratio (S/N), followed by HDI-MSDI, while the lowest ratios are observed for HDI-R and HDI-S. This S/N pattern is opposite to the pattern found for the changes.

A regional analysis of the changes reveals that HDI-R exhibits the largest increase in the probability of compound events in 12, 9, 8, and 9 regions out of the total 20 regions under SSP1-2.6, SSP2-4.5, SSP3-7.0, and SSP5-8.5, respectively (Fig. 2). This is followed by HDI-S, which leads to the greatest increase in the probability of compound events in 8, 10, 11, and 10 regions under the respective scenarios. Conversely, compound events defined based on HDI-P result in the smallest increase in the probability of events in 11, 11, 10, and 11 regions under SSP1-2.6, SSP2-4.5, SSP3-7.0, and SSP5-8.5, respectively.

Overall, the Amazon, Australia, Central America, Mediterranean, southern Africa, South Asia, and Southeast Asia regions are anticipated to experience the most substantial increases in the likelihood of compound hot-dry events (Fig. 2). In the worst-case scenario (SSP5-8.5), the Mediterranean and Amazon regions may experience a potential increase of up to 0.19 and 0.18, respectively, in the probability of compound events. While the magnitude of the increase varies with different scenarios, this growth is however spatially heterogeneous. For example, the Mediterranean region is initially ranked as the fifth most important hotspot region for future compound hot-dry events under SSP1-2.6, but climbs to become the fourth, first, and first most important hotspot under SSP2-4.5, SSP3-7.0, and SSP5-8.5, respectively. Conversely, southern Africa drops from being the second most important hotspot region under SSP1-2.6 to the fourth most important hotspot under SSP5-8.5.

Following the global pattern, significant changes are observed in all regions using all indices; however, HDI-P may not necessarily yield the largest S/N in every region (Fig. 3). When comparing regional S/N across different indices, HDI-P exhibits the highest S/N in 17, 18, 19, and 19 regions out of the total 20 regions under SSP1-2.6, SSP2-4.5, SSP3-7.0, and SSP5-8.5, respectively. In contrast, either HDI-R or HDI-S exhibits the lowest S/N in 75-85% of the regions. For all scenarios, southern Africa shows the largest S/N, even though it is not among the top three hotspot regions in terms of the magnitude of projected changes in compound hot-dry events, highlighting the importance of projection uncertainty. Another example is the Amazon region, which ranks among the top two hotspot regions based on the magnitude of changes but is not even among the top five hotspot regions in terms of S/N.

To account for the sensitivity of the results to the chosen threshold defining compound hot-dry events, the analysis is replicated using two alternative thresholds of −0.9 and −1 within the same threshold range associated with a moderate compound hot-dry condition, in addition to the original −0.8. A comparison of the results reveals similar spatial patterns of changes across different thresholds (Fig. 1; Supplementary Figs. 2 and 3). However, in terms of magnitude, changes tend to decrease when the

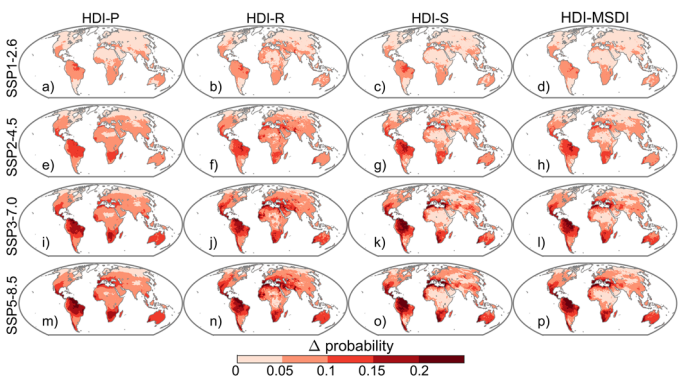

Fig. 1 | CMIP6 ensemble median changes in the probability of compound hot-dry events over the long term (2061–2100) relative to the baseline period (1971–2010) under different scenarios. The figure depicts changes in the probability of compound hot-dry events defined using HDI-P, HDI-R, HDI-S, and HDI-MSDI under the scenarios **a**–**d** SSP1-2.6, **e**–**h** SSP2-4.5, **i**–**l** SSP3-7.0, and **m**–**p** SSP5-8.5. HDI-P, HDI-R, and HDI-S represent the standardized compound hot-dry event index that utilizes respectively precipitation (P), runoff (R), and soil moisture (S) to define dry events. HDI-MSDI represents the standardized compound hot-dry event index that uses all precipitation, runoff, and soil moisture based on a multivariate standardized drought index (MSDI) to define dry events. A compound hot-dry event was defined when HDI < −0.8.

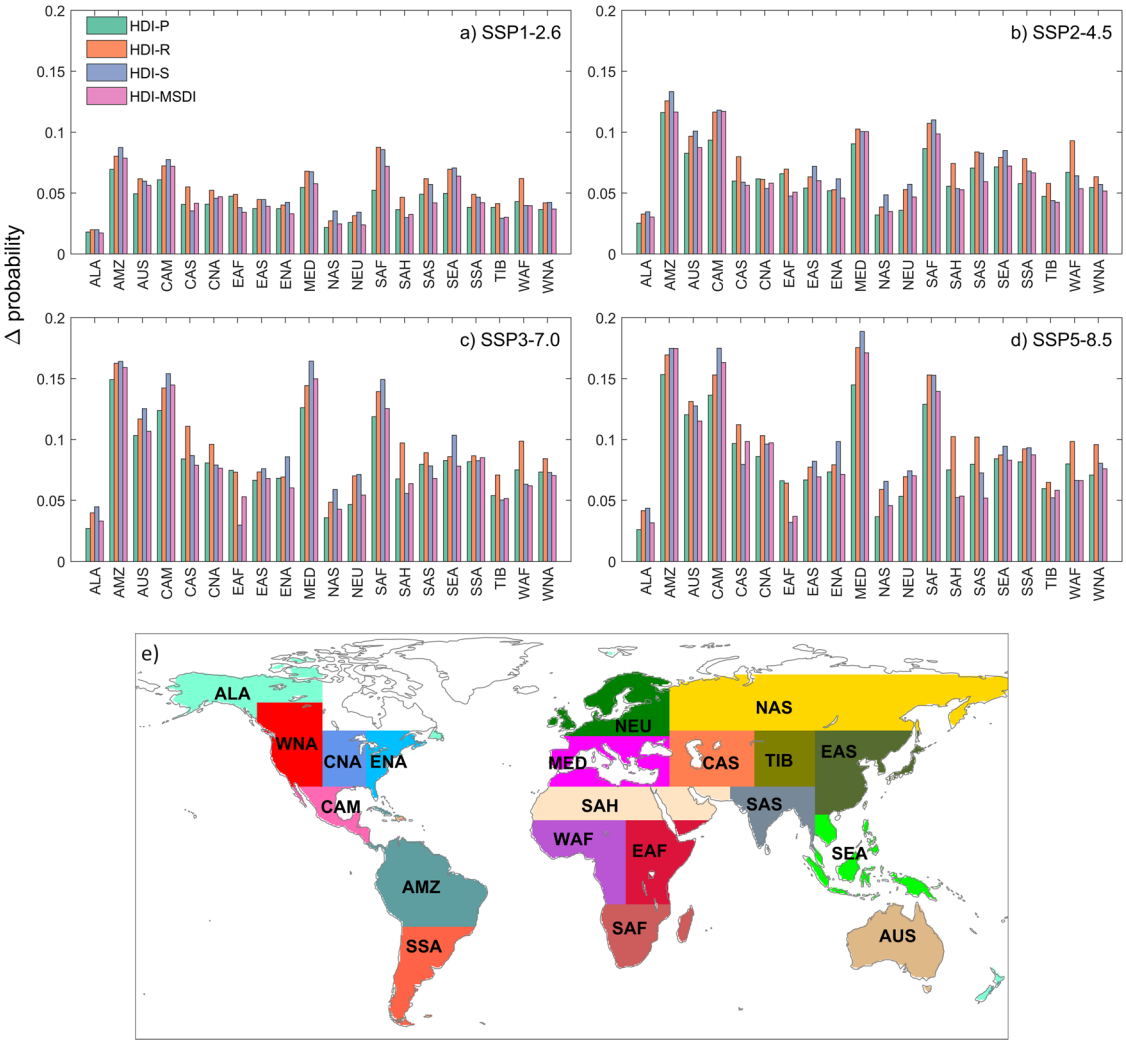

Fig. 2 | Regional comparisons of changes in the probability of compound hot-dry events defined based on HDI-P, HDI-R, HDI-S, and HDI-MSDI under different scenarios. The changes are for the long term (2061–2100) relative to the baseline period (1971–2010) based on the CMIP6 ensemble median for the scenarios **a** SSP1-2.6, **b** SSP2-4.5, **c** SSP3-7.0, and **d** SSP5-8.5. A compound hot-dry event was defined when HDI < −0.8. Figure 2e displays the continental and subcontinental land regions of the globe. ALA: Alaska; AMZ: Amazon basin; AUS: Australia; CAM: Central America; CAS: central Asia; CNA: central North America; EAF: eastern Africa; EAS: east Asia; ENA: eastern North America; MED: Mediterranean basin; NAS: north Asia; NEU: northern Europe; SAF: southern Africa; SAH: Sahara; SAS: south Asia; SEA: southeast Asia; SSA: southern South America; TIB: Tibet; WAF: western Africa; WNA: western North America.

threshold is increased from −0.8 to −1. Regionally, an increase in the magnitude of the change is observed in all regions for all indices (Fig. 4). Specifically, for SSP5-8.5, the change magnitude for the −0.8 threshold is 46–101% larger than that for the −1 threshold. This breaks down to 51–76% for HDI-P, 46–67% for HDI-R, 51–101% for HDI-P, and 50–86% for HDI-MSDI. This pattern remains consistent across other scenarios (Supplementary Figs. 4–6), where the change magnitude for the −0.8 threshold is 45–97% larger than that for the −1 threshold. It is worth noting that the regions experiencing the most substantial changes (e.g., the Mediterranean and Amazon) exhibit the lowest sensitivity to the threshold.

To assess the relative importance of dry indicators for future compound hot-dry event projections, the uncertainty arising from the choice of dry indicators is compared with that stemming from GCMs and scenarios (Fig. 5). GCM uncertainty emerges as the dominant source of uncertainty in 17 out of 20 regions, accounting for an average of 48% across the regions. Scenario uncertainty takes precedence in Central America and the Mediterranean while holding a slight margin in eastern North America: 40.3% for scenario uncertainty compared with 39.8% for GCM uncertainty. In these three regions, the magnitude of the increase in compound event probability escalates rapidly across scenarios, with the increase under SSP5-8.5 being 2-3 times larger than that under SSP1-2.6. On average across the regions, the uncertainty associated with scenarios is 33%, while the uncertainty related to dry indicators for compound events averages at 19%. Notably, the dry indicator uncertainty surpasses the scenario uncertainty in four regions: east and west Africa, South Asia, and Tibet. Additionally, a noticeable uncertainty related to dry indicators (i.e., 27%) is seen in central and north Asia regions.

GCM uncertainty dominates the total uncertainty of compound hot-dry event projections, being the dominant source in 66% of the global land area (Fig. 6). GCM uncertainty of > 40% in compound hot-dry event projections are observed in 69% of the global land area, with 30% of the area showing GCM uncertainty of > 50% (Fig. 7). However, in regions where the expected increases in the likelihood of compound hot-dry events are large, scenario uncertainty is dominant, accounting for 22% of the global land area (Fig. 6). The uncertainty associated with the choice of dry indicators for compound hot-dry events is largest in the Middle East and parts of central Asia and central Africa, accounting for 12% of the global land area (Fig. 6). Scenario uncertainty of > 40% in compound hot-dry event projections is observed in 27% of the global land area, while dry indicator uncertainty of > 40% is seen in 11% of the global land area (Fig. 7).

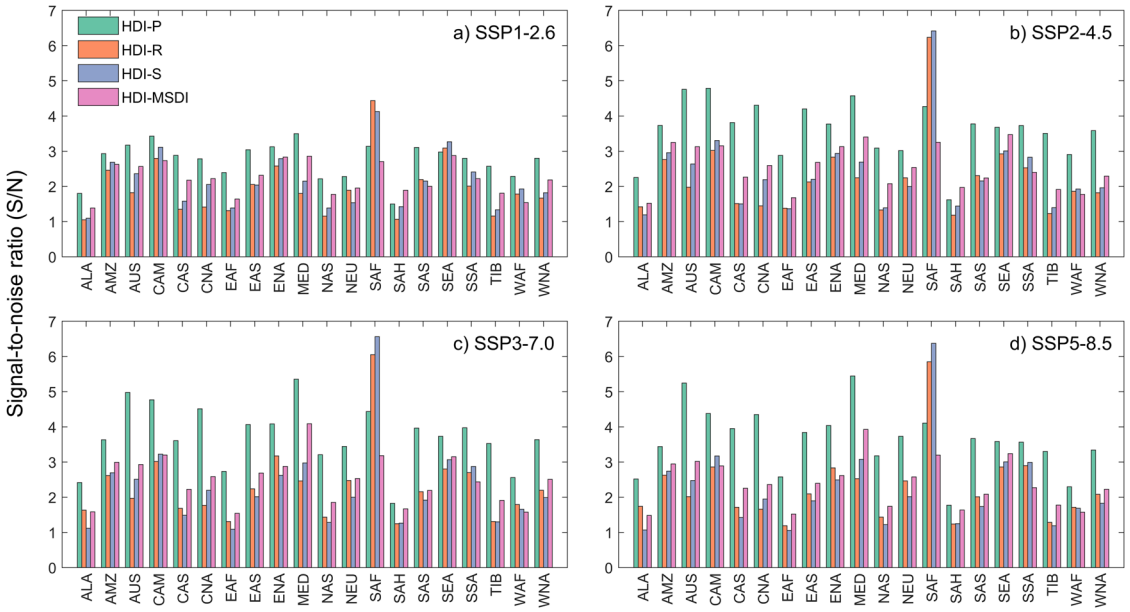

Fig. 3 | Regional comparisons of signal-to-noise ratio (S/N) for the probability of compound hot-dry events defined based on HDI-P, HDI-R, HDI-S, and HDI-MSDI under different scenarios. The changes are for the long term (2061–2100) relative to the baseline period (1971–2010) based on the CMIP6 ensemble median for the scenarios **a** SSP1-2.6, **b** SSP2-4.5, **c** SSP3-7.0, and **d** SSP5-8.5. A compound hot-dry event was defined when HDI < −0.8. See Fig. 2 for the definition of the regions.

Discussion

The discernible intensification of compound hot-dry events, as evidenced through various station, reanalysis, and satellite-based observational datasets, is well-documented in recent studies[3,10,34,36–41]. This growing trend underscores the imperative of scrutinizing these events for their future implications. In this study, we contribute to this line of research by conducting an analysis to examine the evolving likelihood of compound hot-dry events under various future scenarios. Our findings are consistent with prior research, supporting the notion that compound hot-dry events are expected to intensify due to climate change[42–44]. This intensification is particularly evident in regions projected to face severe droughts[15,43,45,46]. When the impacts of dry events combine with the negative effects of hot events, resulting in compound hot-dry events, the overall consequences become even more severe. This means that the negative impacts of hot and dry events reinforce each other, leading to increased risks and potentially more pronounced environmental, ecological, and socioeconomic consequences. The interrelated nature of the physical processes responsible for dry and hot extreme events leads to cascading effects[47], with distinct timescales of interaction, and sensitivity to changes in the soil-plant-atmosphere continuum hydroclimatic drivers, and background aridity[48].

A key focus of this study was the issue of defining dry conditions for compound hot-dry events, which has received limited attention due to being a relatively new frontier in research. In contrast to recent studies that rely on individual hydrological variables to characterize dry events[24,26], we explored the interactions between different hydrological variables and their influence on projections of compound hot-dry events. Our findings demonstrate that using a multivariate index that incorporates precipitation, runoff, and soil moisture to link with air temperature yields different results compared with cases where individual hydrological variables are used. In fact, compound events defined using the multivariate index demonstrate larger changes compared with those defined solely based on precipitation, yet they exhibit smaller changes than those relying on runoff and soil moisture. It is crucial to include these interactions in future projections of compound hot-dry events, given that land-atmosphere interactions are expected to strengthen under warming conditions[49].

Furthermore, our study identified limitations in drought characterization when relying solely on precipitation, such as the Standardized Precipitation Index (SPI). Such an approach overlooks critical land surface and soil conditions that play a substantial role in drought development. Additionally, certain plant processes can influence how precipitation droughts manifest in the soil, such as the reduction in plant stomatal conductance during drought stress or the increased vegetation total water use efficiency under elevated atmospheric CO_2[50,51]. These processes create feedback loops in the near-surface climate that may vary geographically due to variations in vegetation (e.g., phenology, land cover) and land surface properties (e.g., soil moisture content, soil type, topography)[52]. The SPI's inability to incorporate the influencing factors restricts its ability to offer a comprehensive understanding of drought dynamics, especially in regions where these additional variables play a crucial role[33,53]. This becomes particularly relevant in cases where precipitation changes in the opposite direction compared with soil moisture[15,54].

In regions with modest or low climatological precipitation, precipitation alone may not suffice as a measure of drought[55]. Moreover, the precipitation deficit is not a reliable indicator of extreme drought[56]. Extreme drought is often determined by drought intensity, primarily driven by temperature[57]. Higher air temperatures can intensify evaporative demand, leading to increased evaporative losses from the surface and higher soil moisture deficits[58]. A study using GCMs demonstrated that up to 80% of surface rainfall can be lost through evaporation and transpiration, underscoring the substantial impact of temperature on drought severity[59]. Even for characterizing atmospheric water deficit, precipitation may not be the most suitable variable. Due to the limited availability of water for evaporation over land compared with the ocean, land surfaces warm approximately 50% more than ocean surfaces[60], and water vapor content cannot increase rapidly enough to overcome this deficit. Consequently, further drying over land is anticipated as the climate continues to warm[61], leading to an increasing disparity between actual and saturation water vapor concentrations. Therefore, the vapor pressure deficit (VPD), which also governs evapotranspiration demand, is expected to increase much faster by percentage than changes in other hydrological variables, such as precipitation[61,62]. Indices like the Standardized VPD Drought Index (SVDI)[63] may be more appropriate in these situations.

Hence, we caution against relying solely on precipitation-based dry indicators, as it may lead to biased climate change impacts on compound

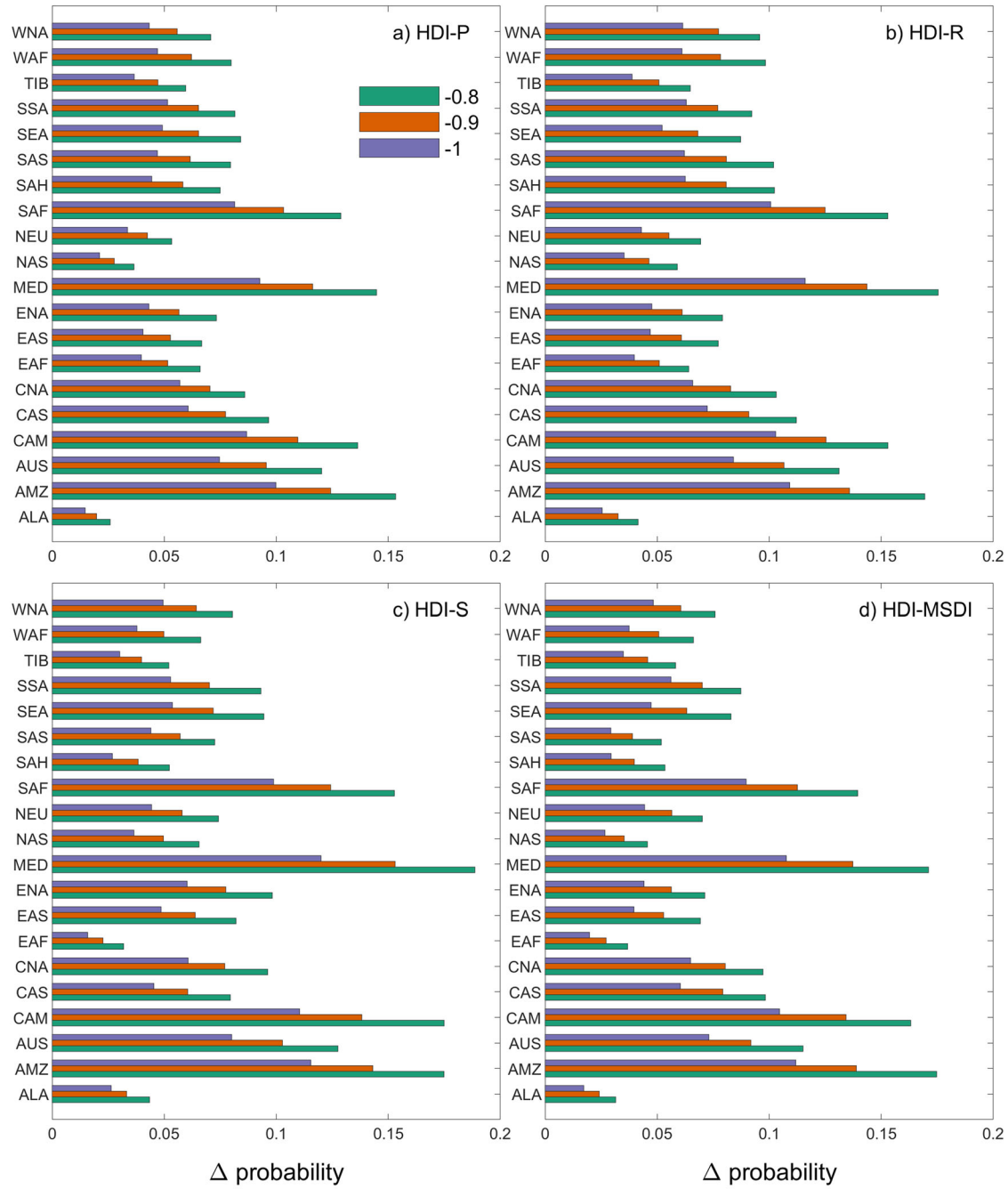

Fig. 4 | Sensitivity of the results to the chosen threshold for defining a compound hot-dry event under the SSP5-8.5 scenario. The figure compares projected changes in the probability of compound events defined using **a** HDI-P, **b** HDI-R, **c** HDI-S, and **d** HDI-MSDI based on three thresholds: −0.8, −0.9, and −1. These changes are evaluated for the long term (2061–2100) relative to the baseline period (1971–2010) using the CMIP6 ensemble median. Refer to Fig. 2 for the definition of the regions.

hot-dry events. Instead, we recommend the inclusion of all pertinent variables in characterizing dry events and considering the interactions between them. Using a multivariate index to characterize dry conditions in compound hot-dry events is advisable, by directly analyzing climate model outputs rather than using a separate offline impact model which is potentially subject to large biases. Compared to precipitation, runoff, and soil moisture can more explicitly represent the core physical processes for drought assessments[50,64]. Our findings indicate that quantifying dry events based on soil moisture yields results closest to those derived from multivariate indices that comprehensively account for interactions between precipitation, soil moisture, and runoff.

Using precipitation to define dry conditions for compound hot-dry events, however, results in lower projection uncertainty and thus a larger S/N compared with the dry event quantification based on runoff, soil moisture, and a multivariate index. This is attributed to the lower uncertainty in precipitation projections compared with runoff and soil moisture projections[15]. In simulating soil and runoff, climate models are required to incorporate soil, landscape, and vegetation attributes alongside climate processes, potentially introducing an additional layer of uncertainty to their projections[65]. Our results show that the compound hot-dry events defined based on HDI-R, HDI-S, and HDI-MSDI inherit this uncertainty, leading to a smaller signal-to-noise ratio compared with the compound hot-dry events defined based on HDI-P.

To assess the relative importance of the characterization of dry conditions for compound hot-dry event projections, we compared the uncertainty arising from the choice of dry indicators with that originating from

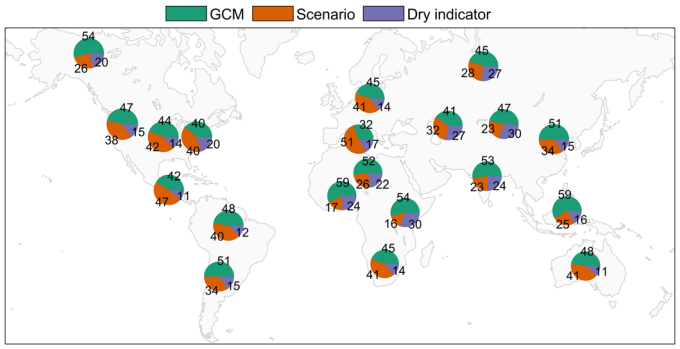

Fig. 5 | Fractional contribution of individual sources to total uncertainty in projected changes in the probability of compound hot-dry events (HDI < −0.8) in the continental and subcontinental regions by 2061–2100 relative to 1971–2010. Dry indicator uncertainty represents the uncertainties associated with the choice of a dry indicator for defining compound hot-dry events. The continental and subcontinental land regions of the globe are shown in Fig. 2e.

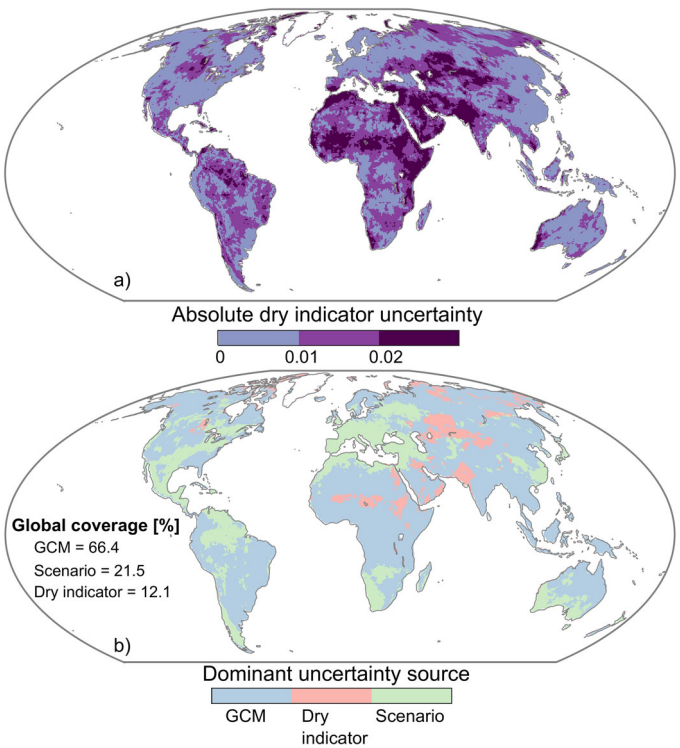

Fig. 6 | Dry indicator uncertainty for compound hot-dry event projections and its importance in relation to other sources of uncertainty. The figure depicts **a** the spatial distribution of absolute uncertainty associated with the choice of dry indicators for compound hot-dry events (HDI < −0.8) and **b** its relative importance compared to uncertainties in GCMs and scenarios. Uncertainties were calculated using the VD-SSS method.

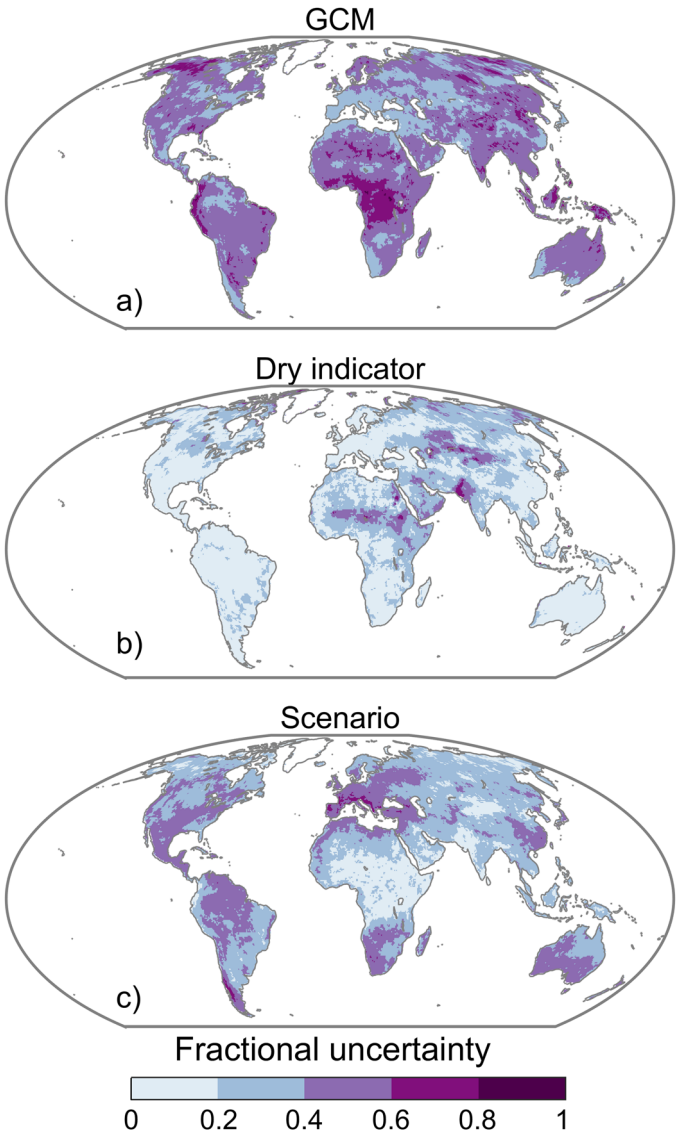

Fig. 7 | Spatial distribution of fractional uncertainties for different sources. The uncertainties associated with **a** GCMs, **b** dry indicators for defining compound hot-dry events (HDI < −0.8), and **c** scenarios were calculated using the VD-SSS method.

GCMs and scenarios. Consistent with previous research on extreme events[27,66,67], we found that GCMs remained the primary source of uncertainty in our study. However, we also observed that the uncertainty associated with the event definition was substantial, reaching up to 30% in certain regions and even surpassing the uncertainty attributed to scenarios. Our study highlights the importance of giving careful attention to the choice of dry indicators when projecting compound hot-dry events, particularly in Africa (east and west Africa) and Asia (north, central, and south Asia, and Tibet). It emphasizes that this aspect should not be overlooked but rather acknowledged as a substantial source of uncertainty that can impact the findings and implications of studies concerning compound hot-dry events.

In addition to the primary focus of this paper, which explores the sensitivity of future compound hot-dry event projections to dry indicators, we also investigated their sensitivity to the chosen threshold for defining such events. Our findings reveal that future compound hot-dry event projections exhibit sensitivity to the chosen threshold. Determining the appropriate threshold entails striking a balance between statistical inference and event extremity[68]. A higher threshold leads to the selection of more extreme events but results in a smaller sample size, introducing bias into statistical analyses. Conversely, a lower threshold detects a greater number of events but leads to less extreme events being included. Hence, selecting the appropriate threshold for defining compound events should be guided by the objectives of impact modeling (e.g., crop modeling, hydrological modeling), while also considering potential statistical biases in the analyses.

While our study offers a quantitative and spatial assessment of the relative impact of the characterization of dry events for compound hot-dry event analyses compared with other sources of uncertainty, there are opportunities for future studies to expand upon this work. Although climate models generally depict historical trends in compound hot-dry events accurately[35,69], their future projections remain subject to uncertainties. Important modeling uncertainties exist for several underlying processes that

drive compound extremes, including changes in aridity[70], land-atmosphere interactions[71], dynamics of snow-atmospheric coupling[72], natural vegetation[51], and precipitation[73]. In our research, we primarily focused on investigating the sensitivity of compound hot-dry event projections and uncertainty to dry indicators. We employed climate model outputs, which directly capture core physical processes like soil moisture and runoff, to characterize dry conditions, enabling a more accurate assessment of the impacts of climate change on dry events[50,64]. However, the World Meteorological Organization (WMO) identified over 50 drought indices based on varying drought indicators (e.g., precipitation, temperature, evapotranspiration)[74]. It would be intriguing to explore how employing commonly used offline impact models, which may be prone to large biases[64], such as the Standardized Precipitation Evapotranspiration Index (SPEI[75]) or the Palmer drought severity index[76], to define dry events would influence the results of compound hot-dry events. Comparing outcomes based on climate model outputs, which directly capture core physical processes, with those derived from offline impact models could offer a more comprehensive understanding of the implications of different dry indicators and the potential biases introduced by using separate offline impact models.

Additionally, future research should explore the effects of defining hot events based on different variables, such as air temperature, dew temperature, and humidity. Different indices that capture these variables could be utilized to define hot events and investigate their influence on the outcomes of compound hot-dry event projections. This would contribute to a more comprehensive understanding of the interplay between different variables and indices in defining compound events. Nonetheless, our study has provided valuable insights into the significance of the dry condition definition for compound hot-dry events and the consideration of interactions between different hydrological variables to capture underlying physical processes and the complexities of events. We have demonstrated that neglecting or underestimating the significance of dry indicators can result in misleading assessments of the potential impacts of climate change on compound hot-dry events.

Materials and methods

Data

Our analysis incorporated precipitation flux (including both liquid and solid phases), total runoff (which includes drainage through the base of the soil model), total soil moisture content (summed water in all phases across all soil layers), and air temperature. To conduct our analysis, we utilized 22 CMIP6 GCMs, including ACCESS-CM2, ACCESS-ESM1-5, BCC-CSM2-MR, CAMS-CSM1-0, CanESM5, CESM2-WACCM, CNRM-CM6-1, CNRM-ESM2-1, FGOALS-f3-L, FGOALS-g3, GFDL-ESM4, INM-CM4-8, INM-CM5-0, IPSL-CM6A-LR, MCM-UA-1-0, MIROC6, MPI-ESM1-2-HR, MPI-ESM1-2-LR, MRI-ESM2-0, NorESM2-LM, NorESM2-MM, and TaiESM1. We analyzed monthly data for precipitation, runoff, soil moisture, and air temperature from these models for both historical simulations and four future tier 1 scenarios (SSP1-2.6, SSP2-4.5, SSP3-7.0, and SSP5-8.5) covering the period 1971-2100 (historical+SSP). These scenarios represent plausible pathways towards different levels of radiative forcing and alternative socioeconomic developments, ranging from sustainable to fossil-fueled development[77]. Our study encompassed the entire global land area grid cells except Greenland due to its perennial snow and ice cover. While compound hot-dry events may not have immediate practical relevance for deserts and hyper-arid regions, they are still useful in providing insights into the potential impacts of climate change.

Quantification of dry events

We characterized dry events using precipitation, runoff, and soil moisture, as well as a multivariate index that combines these variables. For this purpose, we utilized the standardized precipitation index (SPI[78]), the standardized runoff index (SRI[79]), and the standardized soil moisture index (SSI[80]) as dry indicators. The standardized indices were computed for the 3-month time scale, representing seasonal droughts. We employed the Gringorten plotting position to determine the empirical probability of each variable for every month. The resulting probabilities were standardized using the inverse normal transformation to obtain SPI, SRI, and SSI values. Negative SPI, SRI, and SSI values indicate a dry climate condition (drought), whereas positive values signify a wet climate condition. A value close to zero indicates normal climate conditions.

To develop a multivariate standardized drought index (MSDI[80]), for each grid cell of the CMIP6 GCMs, we used copula functions to estimate the joint distribution of precipitation, runoff, and soil moisture. The MSDI is a trivariate index for the 3-month scale of the variables and is expressed as:

$$H(x_1, x_2, x_3) = C(F_1(x_1), F_2(x_2), F_3(x_3)) = C(u_1, u_2, u_3) \quad (1)$$

Here, H is a three-dimensional distribution function of random variables x_1 (e.g., precipitation), x_2 (e.g., runoff), and x_3 (e.g., soil moisture), C is a copula function, and u_1, u_2, and u_3 are variables generated by marginal distribution functions F_1, F_2, and F_3, respectively. Since constructing three-dimensional functions using copulas can be challenging, we used two bivariate copulas to build a three-dimensional function as:

$$C(u_1, u_2, u_3) = C_2(C_1(u_1, u_2), u_3) = p \quad (2)$$

Here, C_1 is the first bivariate copula function that corresponds to variables u_1 and u_2, C_2 is the second bivariate copula function that corresponds to variables $C_1(u_1, u_2)$ and u_3, and p is the joint probability. C_1 and C_2 are of the same type of copula function. We used the Gaussian copula in this study with its parameters estimated by the maximum likelihood method. Previous studies also reported that the differences resulting from the use of different copula functions were negligible when considering changes in drought characteristics and compound hot-dry events at large scales[25,81].

Finally, we computed the MSDI for each grid cell based on the joint probability p (Eq. 2) as:

$$MSDI = \varphi^{-1}(p) \quad (3)$$

where φ is the standard normal distribution function. Similar to SPI, SRI, and SSI, a negative MSDI points to a dry climate condition (drought), while a positive value indicates a wet climate, with an MSDI close to zero denoting normal climate conditions.

Quantification of compound hot-dry events

After characterizing dry events using various methods, we proceeded to quantify compound hot-dry events. To define hot events, we utilized the standardized temperature index (STI[82]). For the detection of compound hot-dry events, we employed bivariate copula functions. We derived the joint distribution probability between the 3-month dry event index, separately for each of the four indices (SPI, SRI, SSI, and MSDI), and monthly STI values[83], using the Gaussian copula. By applying the standard normal distribution (Eq. 3) to transform the remapped joint probability obtained from copula functions, we obtained the standardized compound hot-dry event index (HDI), following the principles of drought indices. We refer to the HDI that uses precipitation (P), runoff (R), soil moisture (S), and MSDI to define dry events as HDI-P, HDI-R, HDI-S, and HDI-MSDI, respectively. To assess climate change impacts, we calculated the changes in the probability of occurrence during the historical (1971–2010) and future (2061–2100) periods. The probability of occurrence for each period was determined by the ratio of instances with a compound event (HDI < −0.8) to the total number of months in each period (40 years x 12 months = 480 months). The threshold of –0.8 corresponds to a moderate compound hot-dry condition, representing the 20th percentile[84]. In contrast to an approach where a compound event is defined only if both margins (dry index and hot index) exceed a specific threshold, our copula-based threshold procedure widens the event space. This procedure incorporates not only events that are jointly marginally extreme but also those that are extreme in the context of the bivariate distribution, even if not necessarily extreme in both margins[85]. Consequently, when both variables fall below an alarm

threshold, HDI leads to a more severe extreme condition than either the dry or hot index alone[80]. To evaluate the impact of varying the threshold settings on the results, we also calculated the probability of compound events using two alternative thresholds of −0.9 and −1 within the same threshold range (−0.8 to −1.2) associated with a moderate compound hot-dry condition[84].

To evaluate the robustness of projected changes in compound hot-dry events, we utilized the signal-to-noise ratio (S/N), as defined by Kendon et al.[86]:

$$S/N = \frac{\bar{y} - \bar{x}}{\sqrt{(\sigma_x^2 + \sigma_y^2)/2}} \tag{4}$$

where an overbar denotes averaging over the ensemble members, and σ_x^2 and σ_y^2 are the variances across the ensemble in the historical (x) and future (y) periods, respectively.

To test the statistical significance of S/N, we applied the t-test. In contrast to the approach of Aalbers et al.[87], who employed a two-sided t-test for precipitation changes, accommodating both increases and decreases, we opted for a one-sided test for compound hot-dry events (HDI), projected to increase globally (see Fig. 1). The significance criterion is given by:

$$\frac{S}{N} \geq t_{n-1,0.05} \times \frac{1}{\sqrt{n-1}} \tag{5}$$

For our sample size of $n = 22$, the critical t-value $t_{n-1,0.05} = 1.72$ and a statistically significant change at the 5% level is indicated by $|S/N| = 0.38$. The critical values for the 1% and 0.1% significance levels are $|S/N| = 0.55$ and $|S/N| = 0.77$, respectively.

Uncertainty analysis

To assess the importance of dry indicators for compound hot-dry events relative to GCMs and SSPs, we used the variance decomposition-same sample size (VD-SSS) method[27] to partition the cascade of uncertainties in compound event changes. This method overcomes the limitations of traditional VD methods, which artificially amplify uncertainty contributions from sources with larger sample sizes[88]. In the VD-SSS iterative sampling-theory based bootstrapping procedure, we used n to denote the smallest sample size among the uncertainty components, which included four sample sizes from dry indicators and SSPs. N represents the size of the largest uncertainty source, which was 22 for the GCM ensemble. After taking the median across the other uncertainty components, we randomly drew n from N and calculated the standard deviation across the bootstrap samples. We repeated this process multiple times (in our case, 1000 iterations) and calculated the median of the empirical bootstrap distribution of sample standard deviation to determine the uncertainty. For the uncertainty component of size n (dry indicator and SSP), we applied the traditional VD method. To determine the fractional uncertainties, we divided the uncertainty of each source by the total uncertainty, which is the sum of the uncertainty contributions (GCMs, SSPs, and dry indicators).

Reporting summary

Further information on research design is available in the Nature Portfolio Reporting Summary linked to this article.

Data availability

The CMIP6 soil moisture, runoff, precipitation, and temperature data used in this study can be accessed online through the Earth System Grid Federation (ESGF) system at https://esgf-data.dkrz.de/search/cmip6-dkrz/. The model output data used to produce Figures are available at https://doi.org/10.5281/zenodo.10878698.

Code availability

The MATLAB codes used in this study are available upon reasonable request from the corresponding author.

Received: 7 November 2023; Accepted: 27 March 2024;
Published online: 24 April 2024

References

1. Miralles, D. G., Teuling, A. J., Van Heerwaarden, C. C. & Vilà-Guerau de Arellano, J. Mega-heatwave temperatures due to combined soil desiccation and atmospheric heat accumulation. *Nat. Geosci.* **7**, 345–349 (2014).
2. Seneviratne, S. et al. Changes in climate extremes and their impacts on the natural physical environment. *Managing the Risks of Extreme Events and Disasters to Advance Climate Change Adaptation: Special Report of the Intergovernmental Panel on Climate Change* 109–230 (Cambridge University Press, 2012).
3. Mukherjee, S., Ashfaq, M. & Mishra, A. K. Compound drought and heatwaves at a global scale: the role of natural climate variability-associated synoptic patterns and land-surface energy budget anomalies. *J. Geophys. Res. Atmos.* **125**, e2019JD031943 (2020).
4. Schumacher, D. L. et al. Amplification of mega-heatwaves through heat torrents fuelled by upwind drought. *Nat. Geosci.* **12**, 712–717 (2019).
5. Miralles, D. G., Gentine, P., Seneviratne, S. I. & Teuling, A. J. Land–atmospheric feedbacks during droughts and heatwaves: state of the science and current challenges. *Ann. New York Acad. Sci.* **1436**, 19–35 (2019).
6. An, W. et al. Anthropogenic warming has exacerbated droughts in southern Europe since the 1850s. *Commun. Earth Environ.* **4**, 232 (2023).
7. González-Herrero, S., Barriopedro, D., Trigo, R. M., López-Bustins, J. A. & Oliva, M. Climate warming amplified the 2020 record-breaking heatwave in the Antarctic Peninsula. *Commun. Earth Environ.* **3**, 122 (2022).
8. Yin, J. et al. Global increases in lethal compound heat stress: hydrological drought hazards under climate change. *Geophys. Res. Lett.* **49**, e2022GL100880 (2022).
9. Alizadeh, M. R. et al. A century of observations reveals increasing likelihood of continental-scale compound dry-hot extremes. *Sci. Adv.* **6**, eaaz4571 (2020).
10. Mukherjee, S. & Mishra, A. K. Increase in compound drought and heatwaves in a warming world. *Geophys. Res. Lett.* **48**, e2020GL090617 (2021).
11. von Buttlar, J. et al. Impacts of droughts and extreme-temperature events on gross primary production and ecosystem respiration: a systematic assessment across ecosystems and climate zones. *Biogeosciences* **15**, 1293–1318 (2018).
12. Ribeiro, A. F. S., Russo, A., Gouveia, C. M., Páscoa, P. & Zscheischler, J. Risk of crop failure due to compound dry and hot extremes estimated with nested copulas. *Biogeosciences* **17**, 4815–4830 (2020).
13. Hao, Y., Hao, Z., Feng, S., Zhang, X. & Hao, F. Response of vegetation to El Niño-Southern Oscillation (ENSO) via compound dry and hot events in southern Africa. *Glob. Planet. Chang.* **195**, 103358 (2020).
14. Pörtner, H. O. et al. *Climate Change 2022: Impacts, Adaptation and Vulnerability*. p. 3056. (IPCC, Geneva, Switzerland, 2022).
15. Hosseinzadehtalaei, P., Van Schaeybroeck, B., Termonia, P. & Tabari, H. Identical hierarchy of physical drought types for climate change signals and uncertainty. *Weather Clim. Extrem.* **41**, 100573 (2023).
16. Reyniers, N., Osborn, T. J., Addor, N. & Darch, G. Projected changes in droughts and extreme droughts in Great Britain strongly influenced by the choice of drought index. *Hydrol. Earth Syst. Sci.* **27**, 1151–1171 (2023).
17. van den Hurk, B. J. et al. Consideration of compound drivers and impacts in the disaster risk reduction cycle. *iScience* **26**, 106030 (2023).
18. Weber, T. et al. Analysis of compound climate extremes and exposed population in Africa under two different emission scenarios. *Earth's Future* **8**, e2019EF001473 (2020).

19. Wu, X. et al. Projected increase in compound dry and hot events over global land areas. *Int. J. Climatol.* **41**, 393–403 (2021).
20. Zhang, G. et al. Climate change determines future population exposure to summertime compound dry and hot events. *Earth's Future* **10**, e2022EF003015 (2022a).
21. Ridder, N. N., Ukkola, A. M., Pitman, A. J. & Perkins-Kirkpatrick, S. E. Increased occurrence of high impact compound events under climate change. *npj Clim. Atmos. Sci.* **5**, 3 (2022).
22. Meng, Y., Hao, Z., Feng, S., Zhang, X. & Hao, F. Increase in compound dry-warm and wet-warm events under global warming in CMIP6 models. *Glob. Planet. Change* **210**, 103773 (2022).
23. Bevacqua, E., Zappa, G., Lehner, F. & Zscheischler, J. Precipitation trends determine future occurrences of compound hot–dry events. *Nat. Clim. Chang.* **12**, 350–355 (2022).
24. Feng, S., Hao, Z., Zhang, Y., Zhang, X. & Hao, F. Amplified future risk of compound droughts and hot events from a hydrological perspective. *J. Hydrol*. **617**, 129143 (2023).
25. Tabari, H. & Willems, P. Sustainable development substantially reduces the risk of future drought impacts. *Commun. Earth Environ.* **4**, 180 (2023).
26. Jha, S., Gudmundsson, L. & Seneviratne, S. I. Partitioning the uncertainties in compound hot and dry precipitation, soil moisture, and runoff extremes projections in CMIP6. *Earth's Future* **11**, e2022EF003315 (2023).
27. Tabari, H., Hosseinzadehtalaei, P., AghaKouchak, A. & Willems, P. Latitudinal heterogeneity and hotspots of uncertainty in projected extreme precipitation. *Environ. Res. Lett.* **14**, 124032 (2019).
28. Lehner, F. et al. Partitioning climate projection uncertainty with multiple large ensembles and CMIP5/6. *Earth Syst. Dyn.* **11**, 491–508 (2020).
29. Hosseinzadehtalaei, P., Tabari, H. & Willems, P. Climate change impact on short-duration extreme precipitation and intensity–duration–frequency curves over Europe. *J. Hydrol.* **590**, 125249 (2020a).
30. Hosseinzadehtalaei, P., Tabari, H. & Willems, P. Satellite-based data driven quantification of pluvial floods over Europe under future climatic and socioeconomic changes. *Sci. Total Environ.* **721**, 137688 (2020b).
31. Wu, Y. et al. Quantifying the uncertainty sources of future climate projections and narrowing uncertainties with bias correction techniques. *Earth's Future* **10**, e2022EF002963 (2022).
32. Satoh, Y. et al. A quantitative evaluation of the issue of drought definition: a source of disagreement in future drought assessments. *Environ. Res. Lett.* **16**, 104001 (2021).
33. Tabari, H., Hosseinzadehtalaei, P., Thiery, W. & Willems, P. Amplified drought and flood risk under future socioeconomic and climatic change. *Earth's Future* **9**, e2021EF002295 (2021).
34. Zhang, Y., Hao, Z., Zhang, X. & Hao, F. Anthropogenically forced increases in compound dry and hot events at the global and continental scales. *Environ. Res. Lett.* **17**, 024018 (2022).
35. Ridder, N. N., Pitman, A. J. & Ukkola, A. M. Do CMIP6 climate models simulate global or regional compound events skillfully? *Geophys. Res. Lett.* **48**, e2020GL091152 (2021).
36. Ridder, N. N. et al. Global hotspots for the occurrence of compound events. *Nat. Commun.* **11**, 5956 (2020).
37. Min, R., Gu, X., Guan, Y. & Zhang, X. Increasing likelihood of global compound hot-dry extremes from temperature and runoff during the past 120 years. *J. Hydrol.* **621**, 129553 (2023).
38. Mukherjee, S., Mishra, A. K., Ashfaq, M. & Kao, S. C. Relative effect of anthropogenic warming and natural climate variability to changes in compound drought and heatwaves. *J. Hydrol.* **605**, 127396 (2022).
39. Wu, H., Su, X. & Singh, V. P. Blended dry and hot events index for monitoring dry-hot events over global land areas. *Geophys. Res. Lett.* **48**, e2021GL096181 (2021).
40. He, Y., Hu, X., Xu, W., Fang, J. & Shi, P. Increased probability and severity of compound dry and hot growing seasons over world's major croplands. *Sci. Total Environ.* **824**, 153885 (2022).
41. Sun, P. et al. Compound and successive events of extreme precipitation and extreme runoff under heatwaves based on CMIP6 models. *Sci. Environ.* **878**, 162980 (2023).
42. Zhang, Q. et al. High sensitivity of compound drought and heatwave events to global warming in the future. *Earth's Future* **10**, e2022EF002833 (2022b).
43. Tabari, H. & Willems, P. Global risk assessment of compound hot-dry events in the context of future climate change and socioeconomic factors. *npj Clim. Atmos. Sci.* **6**, 74 (2023).
44. Batibeniz, F., Hauser, M. & Seneviratne, S. I. Countries most exposed to individual and compound extremes at different global warming levels. *Earth Syst. Dyn.* **14**, 485–505 (2023).
45. Zhao, T. & Dai, A. CMIP6 model-projected hydroclimatic and drought changes and their causes in the twenty-first century. *J. Clim.* **35**, 897–921 (2022).
46. Vicente-Serrano, S. M. et al. Global drought trends and future projections. *Philos. Trans. R. Soc. A* **380**, 20210285 (2022).
47. Sutanto, S. J., Vitolo, C., Di Napoli, C., D'Andrea, M. & Van Lanen, H. A. Heatwaves, droughts, and fires: exploring compound and cascading dry hazards at the pan-European scale. *Environ. Int.* **134**, 105276 (2020).
48. Mukherjee, S., Mishra, A. K., Zscheischler, J. & Entekhabi, D. Interaction between dry and hot extremes at a global scale using a cascade modeling framework. *Nat. Commun.* **14**, 277 (2023).
49. Lesk, C. et al. Compound heat and moisture extreme impacts on global crop yields under climate change. *Nat. Rev. Earth Environ.* **3**, 872–889 (2022).
50. Milly, P. C. & Dunne, K. A. Potential evapotranspiration and continental drying. *Nat. Clim. Chang.* **6**, 946–949 (2016).
51. Mankin, J. S., Seager, R., Smerdon, J. E., Cook, B. I. & Williams, A. P. Mid-latitude freshwater availability reduced by projected vegetation responses to climate change. *Nat. Geosci.* **12**, 983–988 (2019).
52. Lauenroth, W. K., Schlaepfer, D. R. & Bradford, J. B. Ecohydrology of dry regions: storage versus pulse soil water dynamics. *Ecosystems* **17**, 1469–1479 (2014).
53. Manning, C. et al. Soil moisture drought in Europe: a compound event of precipitation and potential evapotranspiration on multiple time scales. *J. Hydrometeorol.* **19**, 1255–1271 (2018).
54. Cook, B. I. et al. Twenty-first century drought projections in the CMIP6 forcing scenarios. *Earth's Future* **8**, e2019EF001461 (2020).
55. Diffenbaugh, N. S., Swain, D. L. & Touma, D. Anthropogenic warming has increased drought risk in California. *Proc. Natl Acad. Sci. USA* **112**, 3931–3936 (2015).
56. Trenberth, K. E. et al. Ch. Observations: Surface and atmospheric climate change. In: *Climate Change 2007: The Physical Science Basis. Contribution of Working Group I to the Fourth Assessment Report of the Intergovernmental Panel on Climate Change* (eds. Solomon, S. et al.) (Cambridge University Press, 2007).
57. Wilhite, D. A. & Glantz, M. H. Understanding: the drought phenomenon: the role of definitions. *Water Int.* **10**, 111–120 (1985).
58. Berg, A., Sheffield, J. & Milly, P. C. Divergent surface and total soil moisture projections under global warming. *Geophys. Res. Lett.* **44**, 236–244 (2017).
59. Abramopoulos, F., Rosenzweig, C. & Choudhury, B. Improved ground hydrology calculations for global climate models (GCMs): soil water movement and evapotranspiration. *J. Clim*. **1**, 921–941 (1998).
60. Dai, A. Recent climatology, variability, and trends in global surface humidity. *J. Clim.* **19**, 3589–3606 (2006).
61. Sherwood, S. & Fu, Q. A drier future? *Science* **343**, 737–739 (2014).
62. Stephens, G. L. & Ellis, T. D. Controls of global-mean precipitation increases in global warming GCM experiments. *J. Clim.* **21**, 6141–6155 (2008).

63. Gamelin, B. L. et al. Projected US drought extremes through the twenty-first century with vapor pressure deficit. *Sci. Rep.* **12**, 8615 (2022).
64. Greve, P., Roderick, M. L., Ukkola, A. M. & Wada, Y. The aridity index under global warming. *Environ. Res. Lett.* **14**, 124006 (2019).
65. Schlaepfer, D. R. et al. Climate change reduces extent of temperate drylands and intensifies drought in deep soils. *Nat. Commun.* **8**, 1–9 (2017).
66. Visser-Quinn, A. et al. Spatio-temporal analysis of compound hydro-hazard extremes across the UK. *Adv. Water Resour.* **130**, 77–90 (2019).
67. Shi, L., Feng, P., Wang, B., Li Liu, D. & Yu, Q. Quantifying future drought change and associated uncertainty in southeastern Australia with multiple potential evapotranspiration models. *J. Hydrol.* **590**, 125394 (2020).
68. Tabari, H. Extreme value analysis dilemma for climate change impact assessment on global flood and extreme precipitation. *J. Hydrol.* **593**, 125932 (2021).
69. Hao, Z., AghaKouchak, A. & Phillips, T. J. Changes in concurrent monthly precipitation and temperature extremes. *Environ. Res. Lett.* **8**, 034014 (2013).
70. Ault, T. R. On the essentials of drought in a changing climate. *Science* **368**, 256–260 (2020).
71. Zhou, S. et al. Land–atmosphere feedbacks exacerbate concurrent soil drought and atmospheric aridity. *Proc. Natl Acad. Sci. USA* **116**, 18848–18853 (2019).
72. Xu, L., & Dirmeyer, P. Snow-atmosphere coupling strength in a global atmospheric model. *Geophys. Res. Lett*. **38**, https://doi.org/10.1029/2011GL048049 (2011).
73. Zhang, B. & Soden, B. J. Constraining climate model projections of regional precipitation change. *Geophys. Res. Lett.* **46**, 10522–10531 (2019).
74. WMO. *World Meteorological Organization (WMO) and Global Water Partnership (GWP) Handbook of Drought Indicators and Indices*. *Integrated Drought Management Programme (IDMP), Integrated Drought Management Tools and Guidelines Series 2*. (eds. Svoboda, M. & Fuchs, B. A.) (WMO, Geneva, 2016).
75. Vicente-Serrano, S. M., Beguería, S. & López-Moreno, J. I. A multiscalar drought index sensitive to global warming: the standardized precipitation evapotranspiration index. *J. Clim.* **23**, 1696–1718 (2010).
76. Wells, N., Goddard, S. & Hayes, M. J. A self-calibrating Palmer drought severity index. *J. Clim.* **17**, 2335–2351 (2004).
77. O'Neill, B. C. et al. The scenario model intercomparison project (ScenarioMIP) for CMIP6. *Geosci. Model Dev.* **9**, 3461–3482 (2016).
78. McKee, T. B., Doesken, N. J. & Kleist, J. The relationship of drought frequency and duration to time scales. In *8th Conference on Applied Climatology* Vol. 17, 179–183 (American Meteorological Society, 1993).
79. Shukla, S. & Wood, A. W. Use of a standardized runoff index for characterizing hydrologic drought. *Geophys. Res. Lett.* **35**, https://doi.org/10.1029/2007GL032487 (2008).
80. Hao, Z. & AghaKouchak, A. Multivariate standardized drought index: a parametric multi-index model. *Adv. Water Resour.* **57**, 12–18 (2013).
81. Tabari, H. & Willems, P. Trivariate analysis of changes in drought characteristics in the CMIP6 multimodel ensemble at global warming levels of 1.5°, 2°, and 3 °C. *J. Clim.* **35**, 5823–5837 (2022).
82. Zscheischler, J. et al. Impact of large-scale climate extremes on biospheric carbon fluxes: An intercomparison based on MsTMIP data. *Glob. Biogeochem. Cycles* **28**, 585–600 (2014).
83. Chiang, F., Greve, P., Mazdiyasni, O., Wada, Y. & AghaKouchak, A. A multivariate conditional probability ratio framework for the detection and attribution of compound climate extremes. *Geophys. Res. Lett.* **48**, e2021GL094361 (2021).
84. Wu, X., Hao, Z., Zhang, X., Li, C. & Hao, F. Evaluation of severity changes of compound dry and hot events in China based on a multivariate multi-index approach. *J. Hydrol.* **583**, 124580 (2020).
85. Brunner, M. I., Gilleland, E. & Wood, A. W. Space–time dependence of compound hot–dry events in the United States: assessment using a multi-site multi-variable weather generator. *Earth Syst. Dyn.* **12**, 621–634 (2021).
86. Kendon, E. J., Rowell, D. P., Jones, R. G. & Buonomo, E. Robustness of future changes in local precipitation extremes. *J. Clim.* **21**, 4280–4297 (2008).
87. Aalbers, E. E., Lenderink, G., van Meijgaard, E. & van den Hurk, B. J. Local-scale changes in mean and heavy precipitation in Western Europe, climate change or internal variability? *Clim. Dyn.* **50**, 4745–4766 (2018).
88. Hosseinzadehtalaei, P., Tabari, H. & Willems, P. Uncertainty assessment for climate change impact on intense precipitation: how many model runs do we need? *Int. J. Climatol.* **37**, 1105–1117 (2017).

Acknowledgements

The authors wish to express their appreciation to the Research Foundation—Flanders (FWO) for funding this work (grant number: 1255423N). The CMIP6 data providers are also acknowledged.

Author contributions

P.H. and H.T. initiated and designed the study. P.H. performed the analysis and wrote the manuscript with input from P.T. and H.T.

Competing interests

The authors declare no competing interests.

Additional information

Supplementary information The online version contains supplementary material available at https://doi.org/10.1038/s43247-024-01352-4.

Correspondence and requests for materials should be addressed to Parisa Hosseinzadehtalaei.

Peer review information *Communications Earth & Environment* thanks Shih-How Lo and the other, anonymous, reviewer(s) for their contribution to the peer review of this work. Primary handling editors: Min-Hui Lo and Aliénor Lavergne. A peer review file is available.